Supporting Information

Hydrogel-based colorimetric assay for multiplexed microRNA detection in a microfluidic device

Hyewon Lee[a], Jiseok Lee[b], Seung-Goo Lee[a,c,*], and Patrick S. Doyle[d,*]

[a]Synthetic Biology and Bioengineering Research Center, Korea Research Institute of Bioscience and Biotechnology, Daejeon 34141, Republic of Korea

[b]School of Energy and Chemical Engineering, Ulsan National Institute of Science and Technology, Ulsan 44919, Republic of Korea

[c]Department of Biosystems and Bioengineering, KRIBB School of Biotechnology, University of Science and Technology, Daejeon 34113, Republic of Korea

[d]Department of Chemical Engineering, Massachusetts Institute of Technology, 77 Massachusetts Avenue, Cambridge, MA 02139, United States

*Corresponding author: P.S. Doyle and S.-G. Lee

E-mail: pdoyle@mit.edu and sglee@kribb.re.kr

Table S1. Probe and target nucleic acid sequences

let-7a probe	5'-Acryd/GAT ATA TTT TAA ACT ATA CAA CCT ACT ACC TCA/InvdT-3'
miR-145 probe	5'-Acryd/ GAT ATA TTT TAA GGG ATT CCT GGG AAA ACT GGA C/InvdT-3'
miR-21 probe	5'-Acryd/GAT ATA TTT TAT CAA CAT CAG TCT GAT AAG CTA/InvdT-3'
let-7a target	5'-UGA GGU AGU AGG UUG UAU AGU U-3'
mir-145 target	5'-GUC CAG UUU UCC CAG GAA UCC CU-3'
miR-21 target	5'-UAG CUU AUC AGA CUG AUG UUG A-3'
biotinylated linker	5'-Phos/TAA AAT ATA TAA AAA AAA AAA A/Bio-3'

Table S2. Detection limit

let-7a	260 fM
miR-145	340 fM
miR-21	242 fM

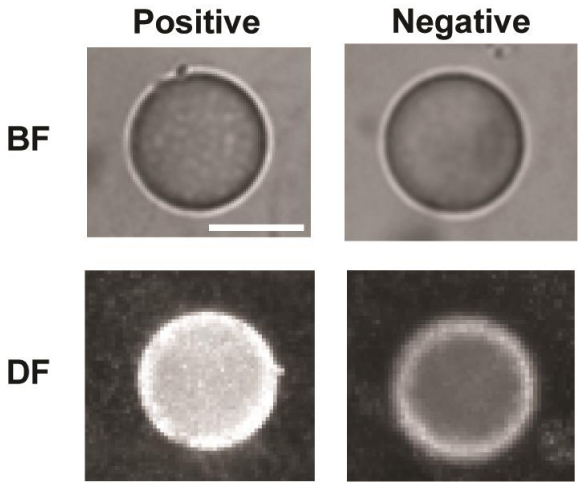

Figure S1. Comparison of bright-field (BF) and dark-field (DF) images. The DF image with the 5 nM of biotinylated probes (positive control) was clearly visualized compared to that with no biotinylated probes (negative control) while BF shows negligible differences. Scale bar represents 100 μm.

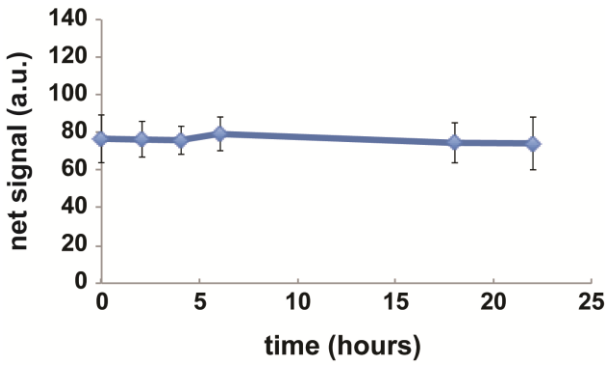

Figure S2. The stability of on-chip hydrogel-based colorimetric assay scheme. There was negligible net signal change over time. The error bars represent the standard deviation (n=6-15).

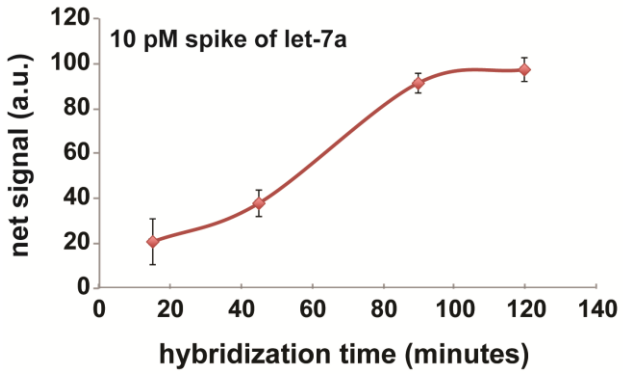

Figure S3. Target hybridization optimization. The net signal increased for up to 90 min of hybridization time. The error bars represent the standard deviation (n=11-15).

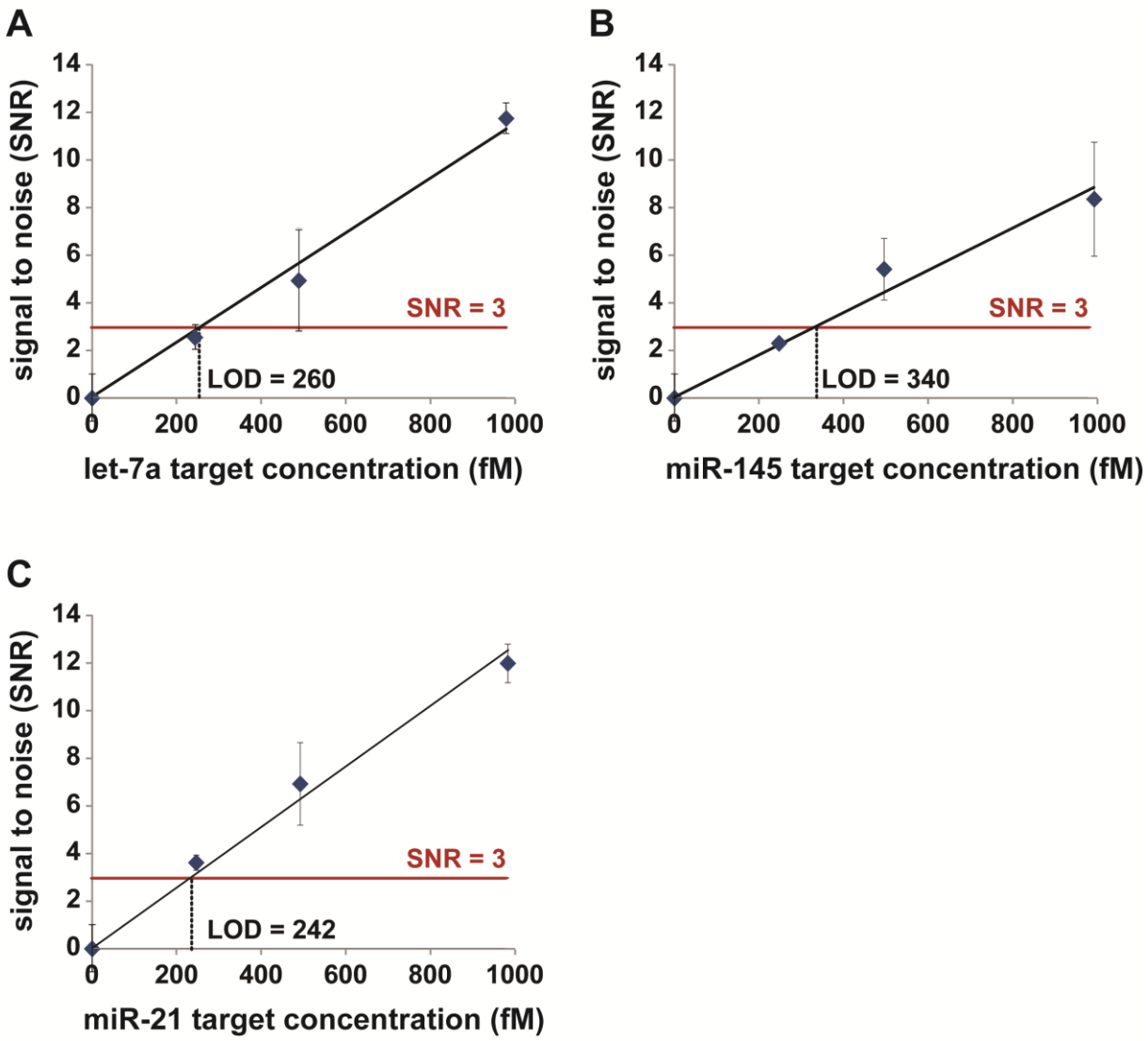

Figure S4. Determination of the limit of detection (LOD) of (A) let-7a, (B) miR-145, and (C) miR-21. The signal to noise ratio (SNR) was plotted as a function of the amount of target miRNAs. The LOD was defined as the target amount where the SNR was three (red line). To calculate the LOD, a line was fit to the data and extrapolated with a mean Pearson coefficient of ~0.99. The LOD was ~260 fM let-7a, 340 fM miR-145, and 242 fM miR-21. The error bars represent the standard deviation of targets normalized by assay noise (n=5-10).

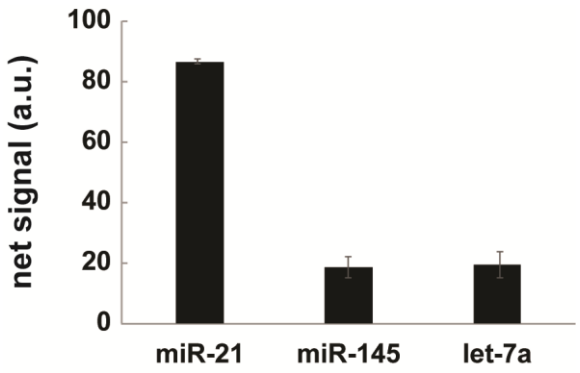

Figure S5. Detection specificity measurement using 10 pM miR-21 target. The minimal interference was observed with miR-145 and let-7a (~ 20% cross reactivity).

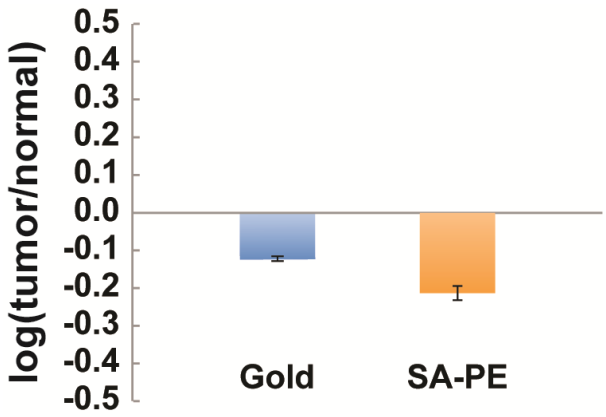

Figure S6. Assay validation of the miRNA assay using total RNA sample. The colorimetric assay based on gold ion deposition was compared to the previously developed assay scheme with a fluorescence label. On comparing the let-7 levels in the heathy versus lung tumor sample, both assays represent a similar dysregulation pattern. The error bars represent the standard deviation of miRNA expression measurements in tumor normalized by background-subtracted average miRNA signal in normal and by the ratio of tumor to normal miRNA expression.